Recognition of Earthquake Prone Areas ($M \geq 6.0$) in the Kopet Dagh Region Using the GIS Technology

***Olga Novikova*[1] *and Alexander Gorshkov*[2*]**

1. M.Sc., Institute of Earthquake Prediction Theory and Mathematical Geophysics, Russian Academy of Sciences, Moscow, Russia
2. D.Sc., Ph.D., Institute of Earthquake Prediction Theory and Mathematical Geophysics, Russian Academy of Sciences, Moscow, Russia,
* Corresponding Author; email: gorshkov@mitp.ru

Received: 02/08/2012
Accepted: 17/11/2013

ABSTRACT

The methodology is based on the idea that large earthquakes correlate with morphostructural nodes which are formed around the intersections of fault zones. The nodes shown on the MZ map of the region under study, have been determined with the morphostructural zoning (MZ) method. The map shows the hierarchical block-structure of the region, the network of boundary zones separating blocks, and the loci of the nodes, formed at the intersections of boundary zones. The GIS facilities have been used to compile the MZ map of the Kopet Dagh region. The recorded earthquakes M6+ nucleate at some of the mapped nodes. The other seismogenic nodes prone to earthquakes M6+ in the Kopet Dagh region have been identified with the help of the pattern recognition algorithm CORA-3. The results obtained indicate a high seismic potential for the studied region and provide information on the loci of potential earthquake sources needed for seismic hazard assessment.

Keywords:
Pattern recognition;
Morphostructural zoning;
Seismogenic nodes;
GIS; Kopet Dagh

1. Introduction

The Kopet Dagh region reveals a high level of seismic activity [1-3]. The goal of this work is to identify sites where earthquakes with $M \geq 6.0$ may nucleate, and define the assemblage of topographic and geological features that discriminate such sites from areas of lower seismic potential.

The methodology used is based on the idea that large earthquakes nucleate at nodes, specific structures that are formed around the intersection of mobile boundary zones separating different blocks of the Earth' crust. In the framework of the methodology, nodes are delineated with morpho-structural zoning method [4]. For identifying earthquake prone areas, the methodology employs the pattern recognition approach, specifically, the recognition algorithm CORA-3 [4-5]. The algorithm discriminates seismo-genic nodes from non-seismogenic ones on the basis of geological-geophysical parameters describing nodes.

The methodology has been systematically tested in many seismic regions of the world including California, Central Asia, Caucasus, Mediterranean, Himalayas and some others (see overview of the problem in [4]). Recent earthquakes of target magnitudes that occurred in previously studied regions have proved the reliability of the methodology: nodes that were recognized in advance as capable of large earthquakes accommodate 84% of the post-publication earthquakes [6].

2. Methodology

The methodology involves two main steps. At the first step with the morphostructural zoning method, we determine the loci of the morphostructural nodes regarded as recognition patterns. At the second step, nodes are divided into nodes where earthquakes with magnitude exceeding a certain threshold (M_0) may occur, and those where only earthquakes with smaller magnitude may happen, using the pattern recognition algorithms CORA-3 [4-5]. For the study region, we have specified $M_0 = 6.0$.

2.1. Morphostructural Zoning Method (MZ)

According to [7], a hierarchical dynamic system of lithospheric blocks and their boundaries is the supporting medium of seismicity. Therefore, delineation of block-and-fault geometry for a seismic region is a necessary stage in studying earthquake prone areas. In order to delineate the block-structure of the Kopet Dagh region, we employ the morphostructural zoning method [4] for the analysis of the present-day topography of the study region. The following characteristics of topography are subject of the analysis: (1) elevation and orientation of large topographic forms and its variations; (2) drainage pattern and its variations; (3) linear elements of topography such as rivers, ravines, escarpments, bottom edges of the slopes of terraces and valleys.

An area is defined as block if: (1) within this area, elevations and orientations of large landforms are homogeneous; (2) drainage pattern is uniform for the entire area. Zones of lineaments are identified at sites where: (1) elevation of topography is sharply changed (1/10 of average elevation within an area); (2) there is narrow strip of topographic alignments having uniform strike; (3) there is sharp turns of predominant strike of large landforms (by 300).

A study region is divided into a system of hierarchically ordered areas characterized by homogeneous present-day topography and tectonic structure. MZ distinguishes (1) areas (blocks) of different rank; (2) their boundary zones, morphostructural lineaments; and (3) sites where lineaments intersect, nodes. Neighboring blocks should differ at least in one of the above characteristics.

MZ is hierarchically ordered and territorial units (blocks) and lineaments are assigned with ranks. Usually, three levels of a hierarchy are considered in MZ. Blocks of the first rank, mountain countries, are divided into blocks of the second rank, megablocks. Megablocks are territories within which all the characteristics of topography are similar or change with a common regularity. Megablocks are further divided into blocks of the third rank, called simply blocks.

A morphostructural lineament is viewed as a boundary zone between territorial units. MZ distinguishes longitudinal and transverse lineaments. Longitudinal lineaments follow the boundaries of large topographic forms. They usually include zones of the prominent faults. Transverse lineaments go across the predominant trend of topography and tectonic structures. Normally, they appear discontinuously on the surface. Zones of transverse lineaments are traced along small individual ridges and/ or chains of small ridges, tectonic scarps, faults, flexures and rectilinear segments of river valleys.

Morphostructural nodes are formed around intersections or junctions of two or several lineaments. Nodes are characterized by a mosaic combination of various topographic forms. The size and geometry of a node can be outlined with fieldwork. If no field investigations were made, a certain circle could be used as a substitute for a node. The radius of the circle depends on the size of earthquakes considered. It should be emphasized that during the compilation of morphostructural map seismicity data have not been taken into account.

2.2. Pattern Recognition Applied to Identification of Earthquake-Prone Areas

The nodes delineated with MZ are viewed as objects of recognition. They are described by topographical, geological, and geomorphic parameters. The values of the parameters form a vector that is associated with a node. Thus, the pattern recognition problem [5] consists of assigning the vectors to two classes: vectors **D** representing nodes where earthquakes with $M \geq M_0$ can occur, and vectors **N** describing nodes where only earthquakes with $M < M_0$ can happen, where M_0 is the target magnitude for a study region. The selection of M_0 depends on seismicity level in the region under consideration.

The classification is known for some objects of recognition on the basis of the seismic activity observed in the region. These objects form a training set of vectors that belong to known classes. The training set consists of vectors $\mathbf{D}_0$ and $\mathbf{N}_0$ that represent, respectively, the nodes where large earthquakes already took place and the nodes situated far from the known large earthquakes. A pattern recognition algorithm provides a division of the vector space into

D and **N**.

Nodes are characterized by a set of parameters. A vector of values of these parameters represents each node. The set of these vectors is the input for the CORA-3 pattern recognition algorithm that we use in this study. Application of the CORA-3 algorithm [4-5] includes the following two stages:

1) Learning stage - selection of the distinctive features of each class on the basis of the training set composed by $\mathbf{D}_0$ and $\mathbf{N}_0$ subsets, which are constituted by all the sample nodes representative of the classes **D** and **N**, respectively;
2) Classification stage - determination of the class to which each node belongs.

The distinctive features (characteristic traits) for classes **D** and **N** are selected at the learning stage. For each node, CORA-3 calculates the number of the characteristic traits for class **D**, the number of those for class **N**, and the difference between numbers of traits. Class **D** includes the nodes for which number of **D** traits exceeds the number of **N** traits.

3. Results

3.1. Morphostuctural Zoning of the Kopet Dagh Region

In order to delineate the block-and-lineament geometry of the study region, we have compiled the morphostructural map at the scale of 1:100,000. The map shown in Figure (1) was compiled using GIS (Geographic Information System) facilities on the basis of joint analysis of topographic, geological, tectonic maps of different scales as well as satellite photos.

The study region has been divided into three mountain countries, these being areal units of the first rank: Kopet Dagh (KD), Allah Dag - Binalud (AD - B) and Quchan-Mashhad (QM), Figure (1). They differ in topography and tectonic evolution. The Kopet Dagh was formed in Neogene-Quaternary, while the Allah Dag - Binalud ranges formed at the margin of the Central Iranian massif in Paleogene-Neogene [9, 11]. The Kopet Dagh consists of a complex system of dissected ranges generally

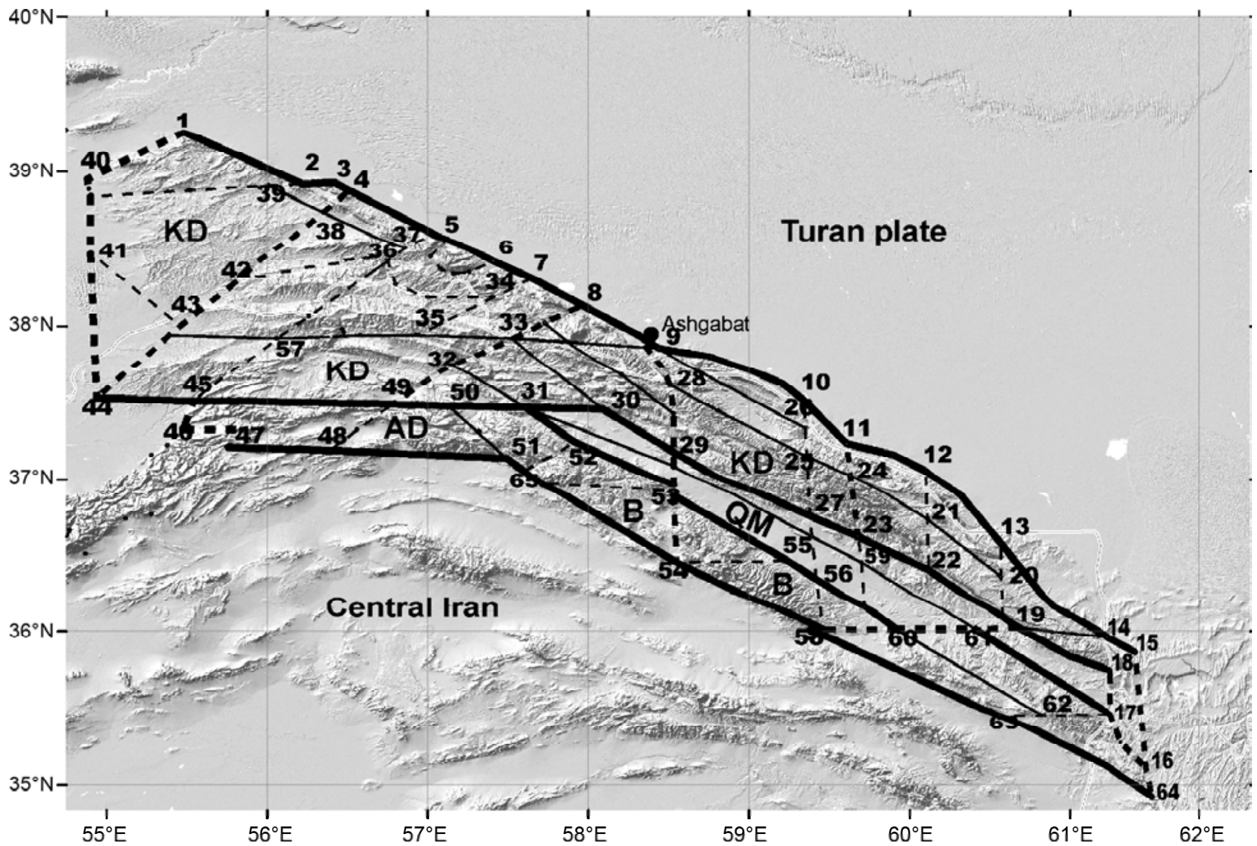

Figure 1. Morphostructural map of the Kopet Dagh region. Thick lines indicate the lineaments of the first rank; medium lines show lineaments of the second rank; thin lines depict the lineaments of the third rank. Continues lines depict the longitudinal lineaments, while the discontinuous ones represent the transverse lineaments. Numerals mark numbers of the nodes. KD - Kopet Dagh, AD - Allah Dagh, B - Binalud, QM - Quchan-Mashhad basin.

trending WNW-ESE, while the Allah Dag - Binalud ranges is composed of more integrated extended ranges forming an arc that is convex northward, Figure (1).

First rank Lineaments. The first rank lineaments separate the study region from the adjacent large-scale tectonic units. In the north, a lineament of the first rank from 1 to 15 separates the Kopet Dagh from the Turan plate. The lineament corresponds to the zone of the complex deepseated South Turkmen fault [8, 9]. In the west, the coastal Caspian lowlands limit the Kopet Dagh near 55E. The boundary between them, lineament from 40 to 44, corresponds to the basement step-faults of N-S orientation [9]. In the south, Kopet Dagh is adjacent to the Quchan-Mashad basin along lineament from 17 to 31. This lineament corresponds to the South Kopet Dagh deep-seated fault [11] and includes the Kashafrud active fault [10]. The lineament from 30 to 44 divides the Kopet Dagh and Allah Dag. The lineament from 16 to 30 separates the Kopet Dagh from Binalud and corresponds to the Atrek-Kashar lineament defined in [9]. The eastern boundary of the Kopet Dagh (lineament from 15 to 64) passes along the southern tip of the Turan plate and belongs to the Urals-Oman superlineament [11].

Megablocks and second rank lineaments. The differences in the elevation and orientation major ranges that compose Kopet Dagh - Allah Dag - Binalud mountain system have determined its division into megablocks. Megablocks are separated from each other by second rank lineaments.

The NE lineament from 4 to 31 was traced along extended straight parts of the Sumbara and Atrek river valleys. The Kopet Dagh Front Range abruptly goes down at the intersection with the lineament zone in a 400-m step. The middle part of this lineament corresponds to a left lateral strike-slip fault exhibiting the lateral offset of 1000 m [11]. The lineament from 8 to 49 is traced along rectilinear parts of several river streams trending northeast. The lineament zone includes steep scarps which terminate the east-west ranges of the Inner Kopet Dagh and corresponds to the NE-SW faults near the city of Kara Kala defined in [9]. The lineament from 9 to 54 zone strikes nearly north-south; its northern part includes the Quchan fault [8-9]. The lineament from 11 to 23 is traced along the extended rectilinear segments of river valleys and scarps that terminate the elevated ranges of the Inner Kopet Dagh.

The present-day relief in the Kopet Dagh heavily dissected. Over the mountain chains, the quantitative index of the topography changes sharply within short distances. Because of this, a dense network of third rank lineaments was delineated by MZ. These lineaments have been traced along the rectilinear parts of river valleys that usually are fault-dominated in young mountains [11]. The third rank lineaments are in good agreement with the faults delineated in [9].

In total, we outlined with MZ 65 intersections of lineaments in the Kopet Dagh region, Figure (1). Each intersection is viewed as a node.

3.2. Nodes and Earthquakes M6+

In this work, we recognize the nodes prone to earthquakes with $M \geq 6.0$. To select the sample nodes for the learning stage of the recognition, we have used the information on the recorded events with $M \geq 6.0$. For this purpose, we analyzed available earthquake catalogs covering the study region [1-3]. The selected shallow earthquakes with $M \geq 6.0$ are plotted in Figure (2).

Since the nodes have been outlined from the cartographic sources without field investigations, their size and shape have not been defined. Here, like in other regions studied with the same methodology for $M_0 = 6.0$ [5], the node is defined as a circle of 25 km of radius, centered at the point of intersection of the lineaments. Such node dimensions are in agreement with the size of earthquake source for the magnitude range considered in this paper. According to [12], the source size of an earthquake with $M = 6.0$ is about 20 km in length and about 10 km in width.

As it can be seen in Figure (2), the epicenters of $M \geq 6.0$ earthquakes recorded in the Kopet Dagh region are located near the intersection of lineaments, i.e. at the nodes. The distance between the epicenters and the points of intersections does not exceed 25 km. We can assume that future earthquakes of the target magnitudes will also correlate with nodes delineated in the Kopet Dagh region, and the pattern recognition technique can pinpoint other nodes capable of earthquakes with $M \geq 6.0$.

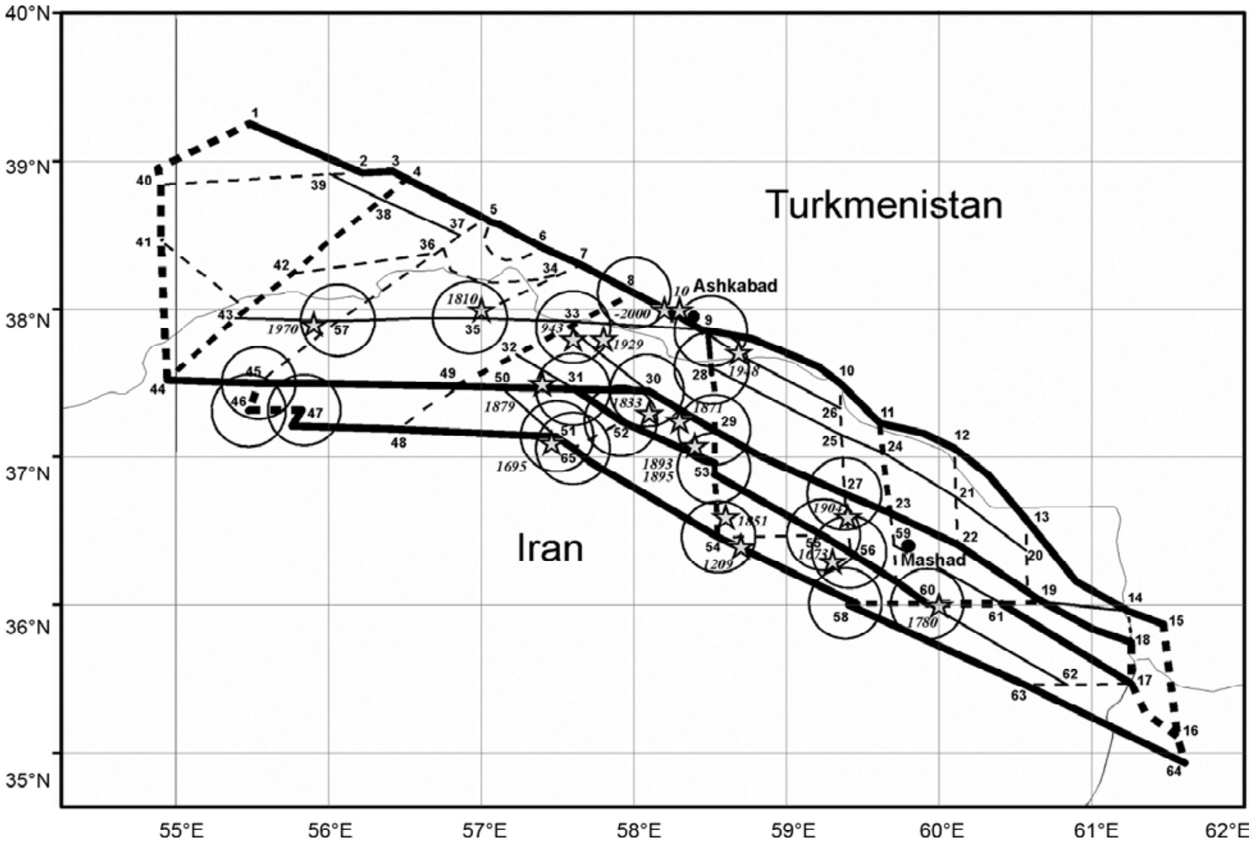

Figure 2. Kopet Dagh region: recognized seismogenic nodes prone to earthquakes with M ≥ 6.0. Lines are the same as in Figure (1). Circles mark D nodes prone to earthquakes with M ≥ 6.0. Stars mark epicenters of earthquakes with M ≥ 6.0. Numerals mark numbers of the nodes.

3.3. Recognition of the Nodes Prone to Earthquakes M6+

The Learning Material: To make up the learning material, the crustal $M \geq 6.0$ earthquakes, including historical ones, Table (1), were selected from regional earthquake catalogs [1-3]. Figure (2) shows that the selected events correlate with some of the nodes. At the learning stage using the information on the recorded $M \geq 6.0$ earthquakes all 65 nodes delineated in the Kopet Dagh with MZ were a priori divided into two sample sets: $\mathbf{D}_0$ representing class **D** and $\mathbf{N}_0$ representing class **N**. The learning set $\mathbf{D}_0$ was made in a formal way. A circle of radius 25 km was drawn around each epicenter shown in Figure (2) and 18 nodes falling in these circles were assigned to the set $\mathbf{D}_0$. These nodes are ## 8, 9, 27, 28, 29, 30, 31, 33, 35, 51, 52, 53, 54, 55, 56, 57, 60 and 65, Figure (2). The rest 47 nodes were included in the sample set $\mathbf{N}_0$.

The Parameters of Intersections of Lineaments Used for Recognition: A uniform parameterization of recognition objects is necessary in order to be able to apply recognition algorithms to them. The set of

Table 1. Earthquakes with M ≥ 6.0.

Year	Latitude, Longitude	Magnitude Ms
2000 BC	38.0N, 58.0E	7.1
10	38.0N, 58.3E	7.1
943	37.8N, 57.6E	7.6
1209	36.4N, 58.7E	7.2
1673	36.3N, 59.3E	7.1
1695	37.1N, 57.5E	7.0
1780	36.0N, 60.0E	6.5
1810	38.0N, 57.0E	6.4
1833	37.3N, 58.1E	6.2
1851	36.6N, 56.6E	6.9
1871	37.2N, 58.3E	7.2
1879	37.5N, 57.4E	6.7
1893	37.1N, 58.4E	7.1
1895	37.1N, 58.4E	6.8
1904	36.6N, 59.4E	6.3
1929	37.8N, 57.8E	7.2
1948	37.7N, 58.7E	7.3
1970	37.9N, 55.9E	6.7

parameters used for recognition is always restricted by their ability to be equally well defined for each node within the area of study. It is for this reason that we have not employed data supplied by instrumental geophysical observations, by space geodesy and so on, even though these could have been helpful for identifying high-seismicity nodes. These data were not available for the entire Kopet Dagh territory. In this work, we use the parameters presented in Table (2), which have been successfully used to recognize high-seismicity nodes in other regions studied [5-6]. The parameter values were determined within circles of radius 25 km around intersections of lineaments using topographic, geological maps, as well as the MZ map for the Kopet Dagh. The parameters incorporate the following data:

1) Information on the contrasts and intensity of tectonic movements based on relief heights around intersections, combinations of landforms, and the area of the soft Quaternary deposits.
2) The indices of tectonic fragmentation for the intersections, which are found directly from the map of morphostructural zoning. These data include the information on the number and ranks of the lineaments that form an intersection.

The CORA-3 pattern recognition algorithm used in this work operates in a binary vector space. Therefore, the values of the parameters were converted into components of the binary vectors by discretization and coding procedure described in [4]. The range of each parameter is divided into two or three intervals by means of a threshold of discretization and then the values of the parameters are converted into binary components 11 ("small"), 01 ("medium") or 00 ("large"), depending upon which interval the value belongs to (the right boundary is included in the interval). The thresholds of discretization were calculated from the condition that the numbers of objects falling into the intervals of discretization are approximately equal. The calculated thresholds of discretization are given in Table (3).

Recognition Results: The nodes have been classified by CORA-3. The algorithm selected 11 **D** traits and nine **N** traits, Table (3), controlling the classification. Of 65 nodes, 22 (34%) are classified **D** and 43 (66%) **N**. All 18 nodes hosting earthquakes with $M \geq 6.0$ are recognized as **D**. Only four nodes (## 45, 46, 47 and 58) originally from $\mathbf{N}_0$ were additionally recognized as **D**. Figure (2) displays the recognized **D** nodes shown by scaled circles in 25 km of radius.

Control Tests: The stability of the resulting classification of the nodes was examined by the control tests that allow evaluating the stability of the node's classification to the changes in the learning sets and in the vector of parameters [4]. In the

Table 2. Parameters used for pattern recognition.

Parameters	Parameters	Thresholds of Discretization
A) Topographic Parameters	Maximum topographic altitude, *m* (H_{max})	1631-2300
	Minimum topographic altitude, *m* (H_{min})	190-615
	Relief energy, *m* (ΔH) (H_{max} - H_{min})	1201-1706
	Distance between the points H_{max} and H_{min}, *km* (L)	35-43
	Slope, ($\Delta H/L$)	38
B) Geological Parameters	The portion of the node area covered by soft (Quaternary) sediments, % (Q)	52
C) Parameters of the Lineament and Blocks Geometry	The highest rank of lineament in a node, (HR)	1
	Number of lineaments forming a node, (NL)	2
	Number of lineaments within a circle of 25 km in radius (NLC)	3
	Distance to the nearest 1st rank lineament, *km,* ($\mathbf{D}_1$)	0
	Distance to the nearest 2nd rank lineament, *km,* ($\mathbf{D}_2$)	32
	Distance to the nearest node, *km,* (D_n)	22-28
D) Morphological Parameter (Mor)	This parameter is equal to one of the following six values in accord with the morphology within each node: 1 mountain and mountain (m/m) 2 mountain and piedmont (m/pd) 3 mountain and plain (m/p) 4 piedmont and plain (pd/p)	

Table 3. Recognized characteristic traits of **D** and **N** nodes in the Kopet Dagh region.

No.	Parameters									
	H_{max} *m*	H_{min} *m*	ΔH *м*	*L* *km*	$\Delta H/L$	Mor	Q %	NLC	D_2 *km*	D_n *km*
	Characteristic Traits of Class **D** (**D**-traits)									
1	>2300						>52			≤ 28
2		>615		≤ 35						≤ 28
3	>2300		≤ 1706							≤ 28
4		>615							≤ 32	>22
5		≤ 190		≤ 35						>22
6		>615					?52		≤ 32	
7		≤ 190	>1706						≤ 32	
8			>1706			m/p or m/pd		≤ 3		
9					>38	m/p		≤ 3		
10	≤ 2300				>38			≤ 3		
11			≤ 1706		>38		≤ 52			
	Characteristic Traits of Class **N** (**N**-traits)									
1			≤ 1706						>32	
2	≤ 2300								>32	
3	≤ 2300						>52			
4	≤ 2300	≤ 615				m/p or m/pd				
5				>35	≤ 38					
6		≤ 615			≤ 38					
7			≤ 1706	>35						
8		≤ 615		>35						
9	≤ 2300			>35						

course of the control tests, we have excluded nodes one by one from learning sets $\mathbf{D}_0$ and $\mathbf{N}_0$ and then we have compared the resulting classification with those obtained in the test performance. The parameters composing the decision rule, Table (3), were also excluded in turn from the recognition. In the classifications obtained in the tests execution 9 nodes changed their belonging to **D** or **N** classes with respect to the resulting classification. According to the empirical criteria developed in [4], such insignificant changes in the resulting classification indicate its sufficient stability.

3.4. The GIS Application

The study has been carried out using GIS technologies at all stages: during preparation and analysis of the initial data for MZ, for the compilation of the MZ map, for the determination of node's parameters and during visualization of the obtained results. On the basis of ARCINFO 10 software [13], a database has been created; the database includes information about regional seismicity, morphostructural lineaments, nodes and their parameters as well as the classification of nodes into **D** and **N** classes.

4. Disscussion and Conclusions

The recognition is claimed successful because 18 nodes hosting the recorded events are recognized as D, Figure (2), i.e. results of the recognition fit the observed earthquakes with $M \geq 6.0$. Four nodes, 45, 46, 47 and 58, where events with $M \geq 6.0$ have not been recorded to date, have been recognized prone to the target earthquakes.

The recognition assigned 22 nodes out of 65 ones to **D** class. The area covered by the recognized seismogenic nodes occupies about 30% of the entire area of the study region. Over the region **D**, nodes form three prominent groups of different size. The largest one occupies the central part of the mountain belt. All nodes composing this group are marked already by earthquakes with $M \geq 6.0$. Five **D** nodes, 27, 55, 56, 58 and 60, form the elongated cluster near Mashhad. Apart from node 58, the other ones accommodate earthquakes of the considered size. Small group of three **D** nodes, 45, 46, 47, is located in the junction zone between the Kopet Dagh, Allah Dag and Alborz. In this area, the Alborz joins the lateral Kopet Dagh - Allah Dag structures at a sharp angle.

Events of the considered size are not known in this area, but the recognition results indicate high seismic potential of this area.

The seismic hazard for the region studied in our work has been evaluated by probabilistic approach in the framework of the GSHAP project [14]. Seismic hazard maps presented in [13] delineate the extended zones of high intensities in the Kopet Dagh region. **D** nodes recognized in our work fall in the zones of high intensities defined in [14]. At the same time, a number of **N** nodes also fall into zones of high intensities. Because of this, our results can be useful for the improvement of the seismic hazard assessment for the Kopet Dagh region. Specifically, the seismic hazard of high intensity zones presented in [14] could be differentiated in more detail.

The distribution of the **D** nodes with respect to lineament rank shows that the overwhelming majority of them is associated with the first and second rank lineaments, i.e. with the boundaries of larger blocks. This is in agreement with the results obtained by the recognition in other regions of the Alpine-Himalayan belt [4, 6].

Additional information to deduce criteria for distinguishing **D** from **N** nodes in the Kopet Dagh region is provided by the characteristic traits reported in Table (3). These traits introduce geomorphic and structural features of earthquake prone areas. In general, Table (3) demonstrates that **D** nodes are characterized by higher degree of the crust fragmentation as compared to **N** nodes. Specifically, **D** nodes are characterized by the "small" distances to the nearest node ($D_n \leq 28$ km) and to the nearest second rank lineaments ($D_2 \leq 32$ km) that suggest an increased fragmentation of the crust around **D** nodes. Additionally, **D** nodes are characterized by "large" values of the slope ($\Delta H/L \geq 38$) that suggest intense vertical movements.

Summing up, we can conclude that the results presented in this paper may contribute to the improvement of the seismic hazard for the Kopet Dagh region.

Acknowledgment

The research has been partly supported by the RFBR (grants 12-05-92699 and 13-05-91167).

References

1. Berberian M. (1994). Natural Hazard and the First Earthquake Catalogue of Iran, Historical Hazards in Iran prior to 1900, **1**, IIEES, Tehran, 605p.

2. Kondorskaya, N., Gorbunova I., Kireev I., and Vandysheva N. (1993). On the Unified Earthquake Catalog of North Eurasia, Seismicity and Seismic Zoning of North Eurasia, Ulomov V. (Ed.), IPE, Moscow, 70-79.

3. Shebalin, N.V. and Tatevosian, R.E. (1997). Catalogue of Large Historical Earthquakes of the Caucasus, Historical and Prehistorical Earthquakes in the Caucasus, Giardini, D. and Balassanian, S. (Ed's), NATO ASI Series, 2, Enviroment, **28**, Kluwer Academic Publishers: Dordrecht/Boston/London, 201-232.

4. Gorshkov, A., Kossobokov, V., and Soloviev, A. (2003). Recognition of Earthquake Prone Areas, Nonlinear Dynamics of the Lithosphere and Earthquake Prediction, Keilis-Borok, V. and Soloviev, A. (Ed's), Springer, Heidelberg, 235-320.

5. Gelfand, I., Guberman, Sh., Keilis-Borok, V., Knopoff, L., Press, F., Rantsman, E., Rotwain, I., and Sadovsky, A. (1976). Pattern Recognition Applied to Earthquake Epicentres in California, *Phys. Earth Planet. Inter.*, **11**, 227-283.

6. Gorshkov, A. (2010). Recognition of Earthquake Prone Areas in the Alpine-Hymalayan Belt, Moscow, Krasand Publisher, 472p, (in Russian).

7. Keilis-Borok, V.I. (1990). The Lithosphere of the Earth as a Nonlinear System with Implications for Earthquake Prediction, *Rev. Geophys.*, **28**, 19-34.

8. Hollingsworth, J., Jackson, J., Walker, R., and Nazari, H. (2008). Extrusion Tectonics and Subduction in the Eastern South Caspian Region Since 10 Ma, *Geology*, **36**(10), 763.

9. Tchalenko, J.S. (1975). Seismicity and Structure of the Kopeh-Dagh (Iran, USSR), Royal Society of London Philosophical Transactions, ser. A, **278**(1275), 1-28,

10. Hessami, Kh., Jamali, F., and Tabassi, H. (2003). Major Active Faults of Iran, IIEES, Tehran.

11. Khain, V.E. (2000). Tectonics of Continents and Oceans, Moscow, Scientific world. 500p, (in Russian).

12. Wells, D.L. and Coppersmith, K.J. (1994). New Empirical Relationships Among Magnitude, Rupture Length, Rupture Width, and Surface Displacement, Bulletin of Seismological Society of America, **84**, 974-1002.

13. ARCGIS 10, License Type: ARCINFO, Copyright 1999-2010 ESRI Inc. All Rights Reserved, http://www.esri.com

14. Balassanian, S., Ashirov, T., Chelidze, T., Chelidze, T., Gassanov, A., Kondorskaya, N., Molchan, G., Pustovitenko, B., Trifonov, V., Ulomov, V., Giardini, D., Erdik, M., Ghavory-Ashtiany, M., Grunthal, G., Mayer-Rosa, D., Shenk, V., and Stucchi, M. (1999). Seismic Hazard Assessment for the Caucasus Test Area, *Annali di Geofisica*, **42**(6), 1139-1151.